# Quantitative ultrasound classification of healthy and chemically degraded ex-vivo cartilage

# Quantitative ultrasound classification of healthy and chemically degraded ex-vivo cartilage

*Angela Sorriento[1,2], Lorena Guachi-Guachi[1,2], Enrico Lenzi [3] , Paolo Dolzani [3], Gina Lisignoli [3], Sajedeh Kerdegari[4,5], Gaetano Valenza[6], Claudio Canale[4], Andrea Cafarelli[1,2], Leonardo Ricotti[1,2]*

*[1] The BioRobotics Institute, Scuola Superiore Sant'Anna, 56127 Pisa, Italy. [2] Department of Excellence in Robotics & AI, Scuola Superiore Sant'Anna, 56127 Pisa, Italy. [3] IRCCS Istituto Ortopedico Rizzoli, SC Laboratorio di Immunoreumatologia e Rigenerazione Tissutale, 40136 Bologna, Italy. [4]Physics Department, University of Genoa, via Dodecaneso 33, 16146 Genoa, Italy. [5]Nanoscopy, Istituto Italiano di Tecnologia, Via Enrico Melen, 83 Edificio B, 16152 Genova, Italy [6]Bioengineerring and Robotics Research Centre E Piaggio, University of Pisa, 56122 Pisa, Italy.[6]Department of Information Engineering, University of Pisa, 56123 Pisa, Italy.*

## Abstract

In this study, we explored the potential of seventeen quantitative ultrasound parameters (radiofrequency-based) in assessing the progressive loss of collagen and proteoglycans (mimicking an osteoarthritis condition) in ex-vivo bovine cartilage samples. The majority of the analyzed metrics showed significant changes as the degradation progressed due to trypsin and collagenase treatment. For the first time, we employed a combination of these ultrasound parameters to create machine learning models for the automated detection of a model of healthy and degraded cartilage samples. A logistic regression model exhibited a remarkable capability of distinguishing between healthy and collagenase-treated cartilage, achieving *accuracy* and an *area under the curve* values of 93% and 90%, respectively. When comparing healthy and trypsin-treated cartilage, an ensemble model yielded *accuracy* and an *area under the curve* values of 83% and 75%, respectively. Histological and mechanical analyses further confirmed the ultrasound findings, as collagenase had more pronounced impact on both mechanical and histological properties compared to trypsin. These metrics were obtained using an ultrasound probe, with a transmission frequency of 15 MHz, typically used for the diagnosis of musculoskeletal diseases. As a perspective, the proposed quantitative ultrasound assessment could become a new standard for monitoring cartilage health, aiding in the early detection of cartilage pathologies and enabling prompt interventions.

## Introduction

The unique properties of articular cartilage are closely linked to the composition and structure of the extracellular matrix, which is mainly composed of a high concentration of proteoglycans (particularly aggrecan), included in a dense network of collagen fibers and water. Proteoglycans endow cartilage tissue with resilience and elasticity, while the collagen network determines its shape and tensile stiffness [1]. Articular cartilage degeneration can occur, due to thraumas or age. Cartilage degeneration is a condition that affects millions of people globally, resulting in pain and functional impairment [2] which lead to long-term complications in the most severe cases, as the onset of osteoarthritis (OA) [3].

Nowadays, the management of articular cartilage degeneration is still an open issue. In addition to novel treatments, there is also need for more sensitive and quantitative methods to facilitate early detection of cartilage lesions, as well as to assess treatment outcomes reliably [4]. Current diagnostic techniques, such as physical examinations, symptom assessments, and conventional radiographs,

often suffer from subjectivity, susceptibility to errors, or radiation exposure. Magnetic resonance imaging is a safe and accurate technique for OA diagnosis; however, it is not routinely used because expensive and time-consuming. Ultrasound (US) offers a promising and safe alternative for cartilage monitoring. However, conventional B-mode imaging examinations primarily provide qualitative and subjective morphological information. Quantitative ultrasound (QUS) techniques work directly on the raw radiofrequency (RF) data, derived from the piezoelectric elements of the ultrasound probe, enabling a quantitative characterization of the examined tissues.

In the existing literature, QUS methods have been explored for the analysis of various soft tissues, trying to correlate the acquired backscattered US signals with alterations in the content and architecture of the tissues [5]. Concerning cartilage, different studies explored the use of high-frequency US ($20\text{MHz} \leq f \geq 50$ MHz) to distinguish between healthy and degraded cartilage [6] [7] [8] [9]. The parameters, typically extracted, include time domain metrics (*e.g.*, speed of sound (SoS), reflection index (RI), surface roughness (URI), thickness) and frequency domain parameters (*e.g.*, attenuation coefficient, integrated backscatter coefficient (AIB), integrated reflection coefficient (IRC)).

Kaleva *et al.* [10] compared time-domain, frequency domain and wavelet transform QUS parameters in terms of their ability to detect degenerative changes in healthy and spontaneously degraded osteochondral samples of bovine patellae, using a transmission frequency equal to 20 MHz. Their results demonstrated that all the analyzed acoustic parameters were capable of detecting degenerative signs; time-domain parameters resulted as sensitive and specific as the more complex frequency-domain or wavelet parameters. Interesting findings were also observed in ex-vivo naturally degraded human articular cartilage [11]. The authors employed high frequency US (29 MHz) to derive thirteen QUS parameters calculated from the normalized spectrum of the RF signals, and effectively able to detect early OA signs. Similarly, a correlation between acoustic parameters (such as URI and RI) and OA grade was also observed in OA-induced animal models, using high-frequency US at 55 MHz [12].

In the studies described above, the degradation process was spontaneous, while in other works the process was chemically induced to better control degradation, by regulating the exposure time to enzymes. Among enzymatic degradation solutions, trypsin is commonly used for simulating the proteoglycan loss during cartilage degeneration, while collagenase is used to mimic the degradation of the collagen network. Wang *et al.* [6], explored high-frequency QUS (40 MHz) to derive URI, AIB, IRC and other acoustic properties of normal and articular cartilage degraded using trypsin (4h) and collagenase (24h). Saarakkala *et al.* [7], also investigated the use of high frequency US (20 MHz), in ex-vivo bovine articular cartilage degraded with collagenase (44h) and trypsin (60 min). The authors found variations in the proposed QUS parameters (RI, URI and spatial variation of US reflection), due to the enzymatic treatments. However, despite the intrinsic high resolution provided by high-frequency US, its possible use in the clinical practice is limited due to the low in-vivo penetration capability.

Only a few studies employed lower frequencies (< 20 MHz) to detect degenerative changes in cartilage tissue. Zhang *et al.* [13] examined the effect of the degradation induced by trypsin at 2h and 4h, using a frequency of 15 MHz. The authors calculated three acoustic parameters (IRC, AIB and averaged magnitude ratio), that were able to detect the loss of proteoglycans. Hattori *et al.* [14] investigated articular cartilage treated with collagenase at different time points of degradation (1h, 2h, 4h, 8h, 16h, 24h), both in-vivo and in-vitro. They calculated the maximum magnitude and echo duration from the wavelet transformation of the RF signal, noting an increase in the maximum

magnitude as the duration of collagenase increased. However, a lack of standardization affects this field. Among the mentioned studies, some authors focused only on the effects of trypsin, while others on collagenase ones, and the time points of degradation vary among different studies.

Recently, we proposed a combination of phase entropy, specifically sample entropy (sampEn) and amplitude information to distinguish between various concentrations of bone mineral content in phantoms mimicking the regeneration of the bone after fracture [15]. We also explored the potential of the sampEn parameter, thickness and RI for discriminating healthy cartilage from cartilage treated with trypsin and collagenase at a single degradation time point [16]. To the best of our knowledge, nobody has systematically investigated the correlation between QUS parameters and the effects of the degradation induced by trypsin and collagenase at different time points, using ultrasound frequencies that can be employed in clinical practice for external US acquisition ($f < 20$ MHz).

In this study, we propose for the first time, a combination of novel quantitative parameters and artificial intelligence algorithms to automatically discriminate healthy from chemically degraded cartilage. Cartilage samples were obtained from healthy bovine condyles, treated with trypsin and collagenase solutions and analyzed at different time points. Three time points were chosen for the measurements: for the trypsin treatment, t=0h (control), t=2h (moderate degradation) and t=4h (severe degradation) were set; for the collagenase treatment, t=0h (control), t=6h (moderate degradation) and t=24h (severe degradation) were set. RF data were acquired using a transmission frequency of 15 MHz and analyzed offline to derive quantitative diagnostic metrics. Mechanical analyses and histological evaluations were performed to confirm the differences found in the different cartilage samples.

## Results

### Ultrasound measurements and data analysis

The values of the seventeen QUS metrics extracted from the RF signals at the different time-points are shown in Figure 1 for the trypsin and in Figure 2 for the collagenase treatment (for further details regarding the metrics calculation, please refer to the appendix section (a) in the supplementary material). The explored QUS metrics were grouped into three distinct sub-datasets: complexity and irregularity, cartilage features, and compressed features (see Materials and Methods section).

*Complexity and irregularity*

In Figure 1a and Figure 2a, the eight metrics indicating the complexity and irregularity of the RF signals are reported. All the parameters, except the *mean crossing* and *spectral entropy*, exhibited significant variations after 4h of trypsin treatment (Figure 1a). *Approximate entropy (ApEn), sample entropy (sampEn), mean crossing, Katz fractal dimension* and *$50^{th}$ percentile* changed significantly between 2h and 4h of trypsin treatment. *Mean crossing* was able to discriminate also the first sign of trypsin-induced degeneration, showing a difference between 0h and 2h. Regarding collagenase treatment, all the analyzed parameters, except for *spectral entropy*, *std* and *kurtosis* exhibited significant differences between 0h and 24h. All the parameters, with the exception of *spectral entropy* and *std* showed a significant variation between 0h and 6h. *SampEn* and *mean crossing* revealed differences between 6h and 24h of treatment.

*Cartilage features*

In Figure 1b and Figure 2b, the four parameters closely associated with the cartilage structure, are reported. The RI at the water-cartilage interface ($RI_c$) significantly decreased with cartilage degeneration progression induced by collagenase. The RI at the cartilage-bone interface ($RI_b$)

significantly varied with trypsin degradation, while no changes were found in collagenase treatment. The *bone propagation* revealed considerable alterations after both treatments at different time points of degradation, except between 0h and 4h of trypsin digestion. *Cartilage length* showed a significant decrease at each time point during collagenase degradation, whereas a significant difference was observed only after 4h of trypsin treatment. In addition, the cartilage thickness can be derived from the *cartilage length* by determining the time of flight and the SoS of healthy cartilage and degraded cartilage (for further details, please refer to the appendix section (a) in the supplementary material). The cartilage thickness was 1.61 ± 0.40 mm at 0h, 1.60 ± 0.42 mm after 2h and 1.49 ± 0.24 mm after 4h of trypsin treatment. Concerning collagenase, the thickness was 1.98 ± 0.74 mm at 0h, 1.50 ± 0.59 mm after 6h and 0.57 ± 0.30 mm after 24 h of cartilage treatment.

*Compressed features*

Finally, in Figure 1c and Figure 2c, the compressed features derived from RF data by using encoder layers (Figure S1a) are presented. No significant changes were observed in the *F1* and *F4* features for samples after trypsin treatment. Similarly, no significant variations were evident in the *F1* and *F2* features for samples subjected to collagenase treatment. For trypsin treatment (Figure 1c), the *F2* feature revealed significant changes between samples treated at 2h and 4h; the *F3* feature indicated significant differences between 0h and 2h; while the *F5* feature evidenced changes after trypsin treatment, both between samples treated at 0h and 4h, and between samples treated at 2h and 4h. Regarding collagenase treatment (Figure 2c), the F3, F4 and F5 features showed significant changes between 0h and 6h of treatment. Both the F3 and *F4* features revealed significant distinctions between samples treated for 6h and those treated for 24h; while *F4* also confirmed significant differences between 0h and 24h.

All the results of the QUS parameters in terms of median ± interquartile range are reported in Table S1.

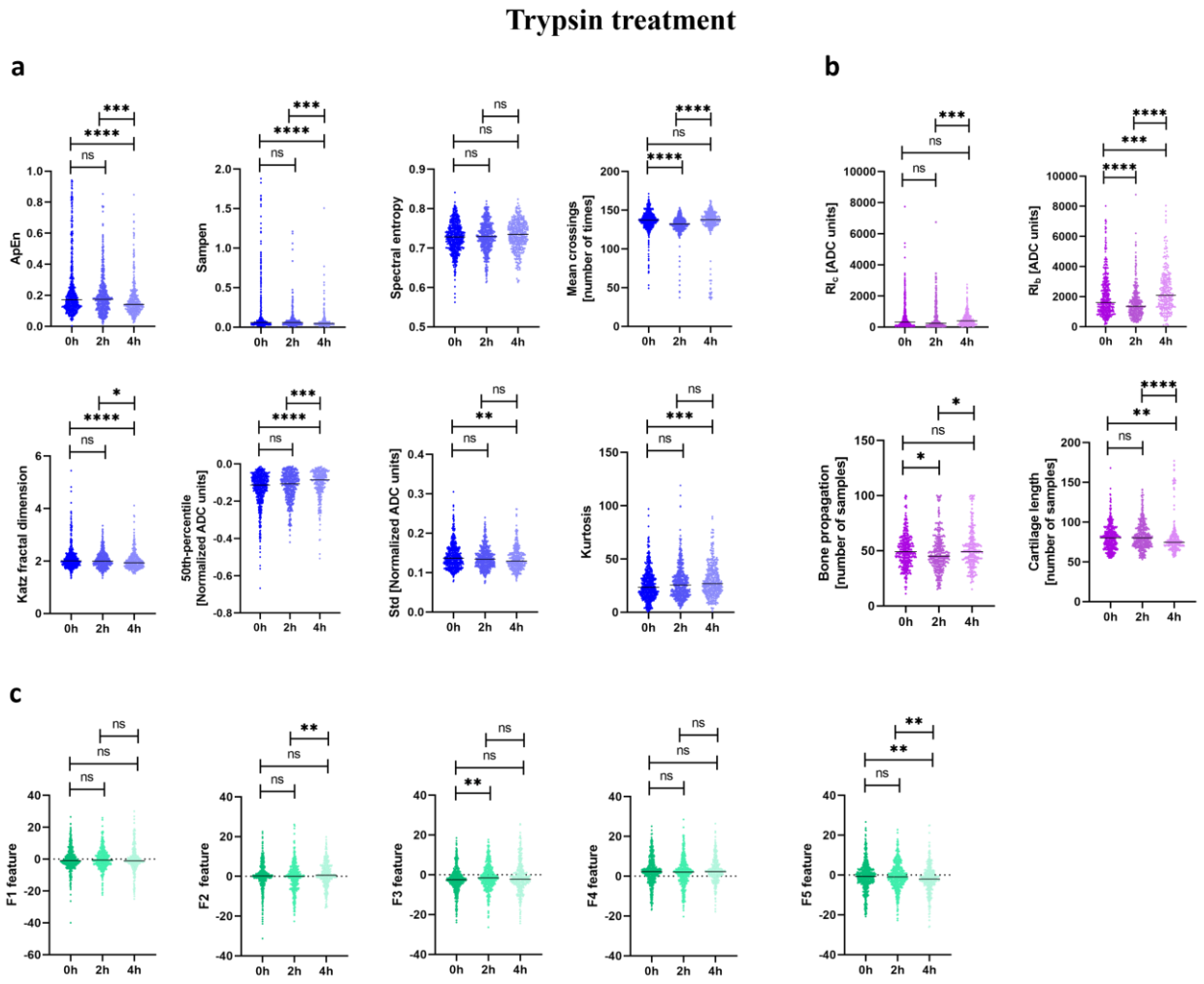


Figure 1. QUS metrics of cartilage samples treated using trypsin: complexity and irregularity parameters (a), cartilage features (b), and compressed features (c). Kruskal-Wallis was used for multiple comparisons, whereas Dunn's test was used as post-hoc analysis. * $p<0.05$, ** $p<0.01$, *** $p<0.001$, **** $p < 0.0001$.

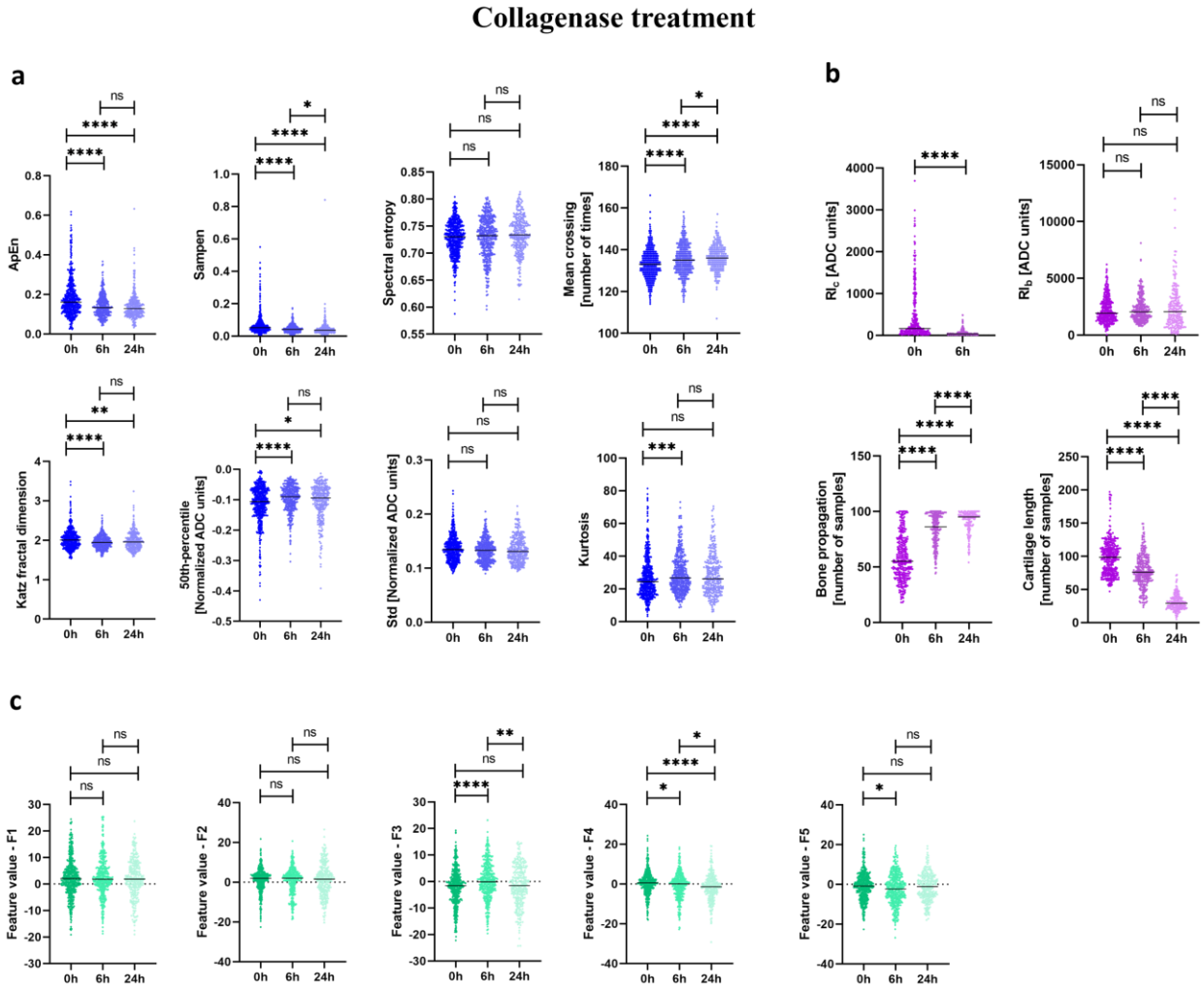


Figure 2. QUS metrics of cartilage samples treated using collagenase: complexity and irregularity parameters (a), cartilage features (b), and compressed features (c). Kruskal-Wallis was used for multiple comparisons, whereas Dunn's test was used as post-hoc analysis. * $p<0.05$, ** $p<0.01$, *** $p<0.001$, **** $p < 0.0001$.

*ML-based classification*

In this study, Machine Learning (ML) models were also tested to discriminate between two classes (healthy and degenerated) for each enzyme treatment. Specifically, samples treated with trypsin at 2h and 4h were grouped as "trypsin degeneration" and samples treated with collagenase at 6h and 24h were grouped as "collagenase degeneration". A preliminary analysis was conducted to identify the contribution score of each feature in the classification of cartilage degeneration, enabling effective discrimination between healthy and degenerated samples. The results are presented in Figure S2 of the supplementary material. These QUS metrics were used to automatically distinguish healthy and chemically degraded samples using ML models. We tested these models in our $\text{Test}_{\text{MLmodel}}$ datasets, consisting of 5 healthy and 10 degraded samples for both trypsin and collagenase treatments.

Table S2 and Table S3 report the overall effectiveness of the most proficient ML models trained on our $\text{Training}_{\text{MLmodel}}$ datasets. The ML models were trained and evaluated 10 times (see results in Table S4 and Table S6 in the supplementary material). From these results, it was observed that the ensemble and logistic regression methods showed the highest *accuracy* and *area under the curve (AUC)* values for trypsin (80, 75) and collagenase (93, 90), respectively. In fact, a closer examination of the test confusion matrices (Figure *3*) for the ensemble model, used for trypsin treatment, showed

that only two healthy samples were misclassified as degenerated and, conversely, just one degenerated sample was incorrectly classified as healthy. In the regression model used for collagenase treatment, only one healthy sample was incorrectly classified as degenerated.

Furthermore, the results for identifying the three classes of degradation (healthy, moderate and severe) are reported in the supplementary material (Figure S3, Table S5, Table S7). In this case, the limited amount of available training data (33 samples on 3 classes for trypsin and 27 samples on 3 classes for collagenase) influences the performance of the classification results, decreasing 28% of *accuracy* value for trypsin and 21% of *accuracy* value for collagenase.

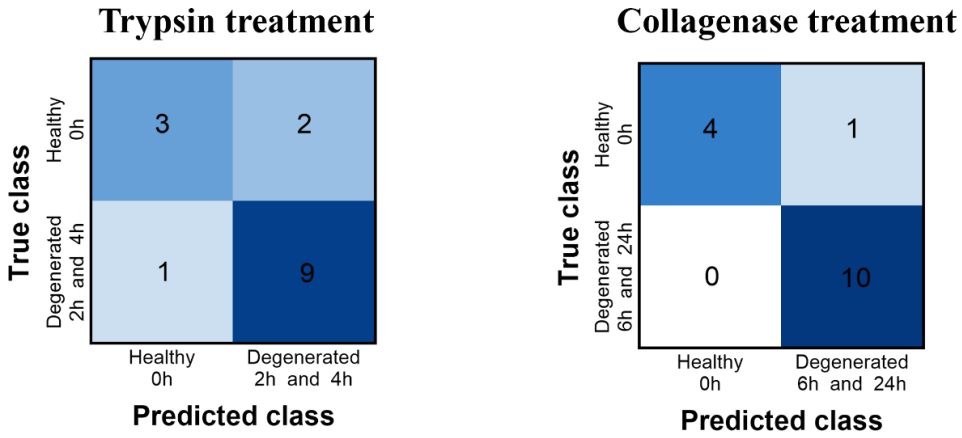


Figure 3 – Confusion matrices relative to the ensemble and logistic regression models for trypsin and collagenase treatments.

**Histologic analysis**

*Trypsin treatment*

Safranin O positive staining evidenced a progressive and significant decrease in proteoglycan content over time after trypsin treatment (Figure 4a, b). Before trypsin treatment (0h), the cartilage area was 100% positive for the staining. After 2 hours of treatment (2h), the positive surface area decreased approximately down to 80 % of the total cartilage area, and after 4 hours (4h), the positivity dropped almost to 0%. Only in a few cases, we observed a very small residual positive area (<5%) (Figure 4b). Quantification of Safranin O positive areas evidenced a significant decrease after trypsin treatment both at 2h and 4h but also between these two time points (Figure 4b). By contrast, Picrosirius Red staining showed the preservation of collagen fibers within the cartilage even after 4 hours of treatment (Figure 4c, d), indicating that the collagen network was not affected by trypsin treatment along the cartilage thickness (100% positive staining).

*Collagenase treatment*

In the sample stained with Safranin O, collagenase treatment showed a progressive and significant decrease in proteoglycan content over time (Figure 4e, f). The positive surface area, which corresponds to 100% of the cartilage before degradation (0h), evidenced a significant decrease of approximately 65% after 6 hours (6h), evidencing a substantial reduction in proteoglycans and alterations of the superficial zone. On the other hand, the Picrosirius Red staining (Figure 4g, h) also confirmed this trend, showing a reduction of collagen content from 100% at 0h to 70% after 6h. After 24 hours (24h) of collagenase treatment, we observed a complete depletion of the cartilage matrix.

We noted only in a few samples the presence of the cartilage deep layer attached to the subchondral bone. Collagenase treatment significantly impacted the whole structure and thickness of the cartilage.

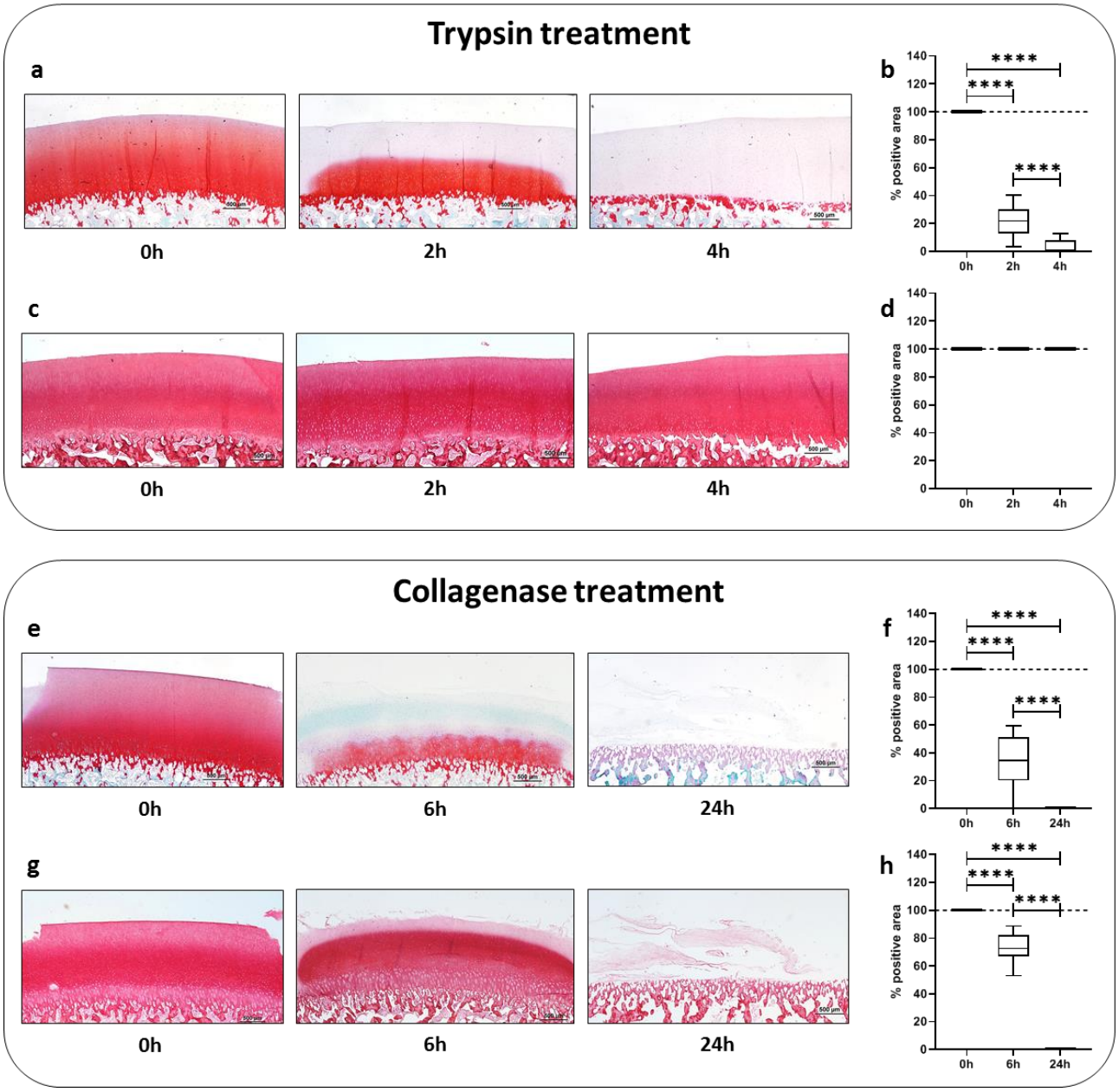


Figure 4. Representative histological images of Safranin O (a) and Picrosirius (c) Red-positive stained area of the cartilage treated with trypsin at three different time points (0h, 2h and 4h) with the corresponding quantification of cartilage positive area (b, d, respectively), and representative histological images of Safranin O (e) and Picrosirius (g) Red-positive stained area of the cartilage treated with collagenase at three different time points (0h, 6h and 24h), with the corresponding quantification of cartilage positive area (f, h, respectively). Quantification of cartilage positive area (b, d, f, h) are represented as Box-plot with median, minimum and maximum. Kruskal-Wallis with Dunn's multiple comparisons test was used for statistical analysis: **** $p < 0.0001$.

## AFM indentation

In Figure 5 the elastic moduli obtained through Atomic Force Microscopy (AFM) indentation experiments are shown for cartilage before and after trypsin and collagenase treatments. The results revealed a marked decrease in the mechanical properties after both trypsin and collagenase

treatments. The softening effect of collagenase treatment was particularly effective. Cartilage samples resulted particularly sticky after the complete depletion of collagen, making AFM analysis a challenge (see also Figure S4 in the supplementary material).

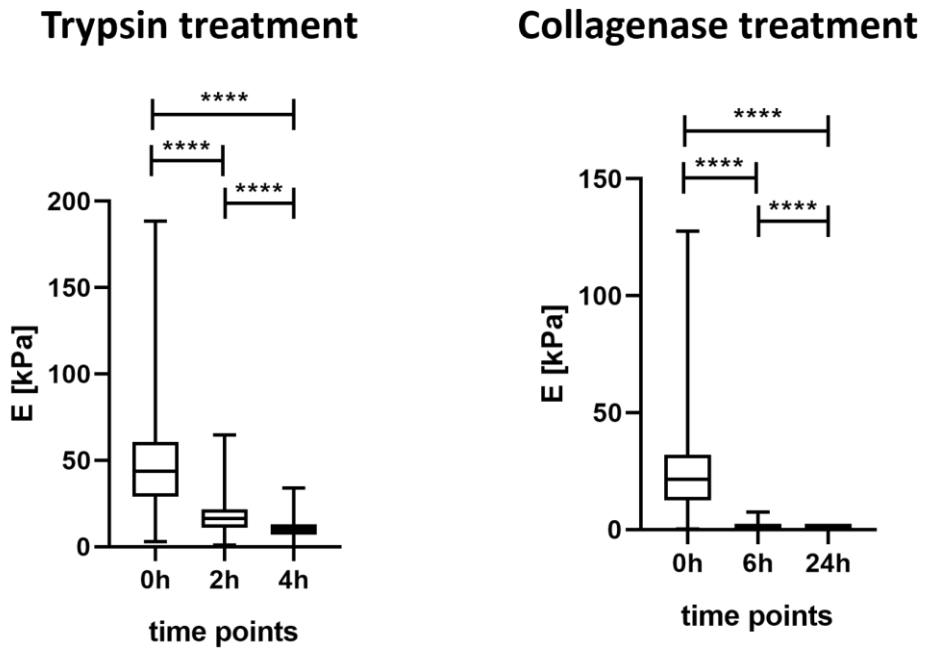


Figure 5. Elastic modulus calculated on samples treated with trypsin and collagenase. Kruskal-Wallis was used for multiple comparisons, whereas Dunn's test was used as post-hoc analysis. **** $p < 0.0001$.

## Discussion

In this study, healthy cartilage samples were extracted from bovine condyles and subjected to enzymatic degradation using trypsin and collagenase to simulate the loss of proteoglycans and collagen networks, occurring during articular cartilage degenerative pathologies, such as OA. Three time points were established for assessing the outcomes of both enzymatic treatments, simulating healthy cartilage, moderate degeneration and severe degeneration.

A total of seventeen QUS metrics have been extracted from the raw RF signals with the aim to discriminate the different degrees of degeneration, induced by the two enzymes. Overall, the features varied significantly after both treatments and some metrics were more sensitive than others in detecting even early signs of degradation (Figure 1 and Figure 2).

*Complexity and irregularity*

In Figure 1a and Figure 2a, quantitative features describing the complexity and irregularity of the time-series signals, are reported. *ApEn*, *sampEn* and *spectral entropy* have already been widely employed for estimating the randomness of EEG signals [17], [18]. *Std*, *50-percentile*, and *kurtosis* have been extensively studied for the characterization of physiological signals [19], [20], while *mean crossings* have found application in the characterization of voice pathologies [21]. *Katz's fractal dimension* has been used in previous works as a tool for analyzing the complexity of biomedical waveforms, for example in sleep electroencephalograms [22]. The potential of all these metrics for characterizing cartilage samples, based on RF data, has never been explored, except for *sampEn*, which was preliminarily investigated by the authors as a metric to discriminate between healthy and degenerated cartilage [16]. In this study, both *ApEn* and *sampEn* decreased significantly after

enzymatic treatments, indicating an increase in the regularity of the time series due to the decomposition of the cartilage matrix, which is inherently characterized by high inhomogeneity across its thickness [2]. *Spectral entropy* was not affected by trypsin and collagenase degradation, suggesting no differences in the uniformity of energy distribution. *Mean-crossings* and *50-percentile*, increased significantly after both trypsin and collagenase digestion. The *mean-crossing* results demonstrated that the degeneration action leads to an increase in the number of vibration patterns, which is an indicator of joint pathology [23]. Results from *50-percentile* measures indicated that the degradation action increases the middle-value trends of the signals. *Std* measures decreased after both treatments, showing significant differences for trypsin treatment and suggesting a lower signal fluctuation around the mean value, after cartilage degeneration. In agreement with the decrease of *std*, *kurtosis* increased significantly, demonstrating that the degradation action resulted in values more concentrated in a narrow range. Katz's fractal dimension showed a significant decrease after severe degradation actions caused by trypsin (0h-4h, *$p<0.05$) and collagenase (0h-24h, *$p<0.05$), suggesting a reduction in waveform complexity after the treatments. The results demonstrated the ability of Katz's fractal dimension also to discriminate slight changes induced by trypsin (2h-4h, *$p<0.05$) and collagenase (0h-6h, *$p<0.05$). Overall, these metrics were able to detect changes in the complexity and regularity of the RF signals from both healthy and chemically degraded cartilage samples. In general, the degradation process resulted in less complex and more regular signals, with values characterized by lower dispersion.

*Cartilage features*

Figure 1b and Figure 2b report the results of the parameters strictly related to the cartilage samples structure: *i)* $RI_c$ at the water-cartilage interface, *ii)* $RI_b$ at the cartilage-bone interface, *iii) cartilage length* (in terms of the number of samples between the water-cartilage interface and the cartilage-bone interface), *iv) bone propagation* (in terms of number of samples between the bone interface and the last peak in the RF signal). Ideally, we would expect $RI_c$ and *cartilage length* to decrease and $RI_b$ and *bone propagation* to increase as the degradation progresses. Indeed, as the cartilage degrades, the difference in acoustic impedance decreases at the water-cartilage interface and increases at the cartilage-bone interface. We observed minor changes in the samples treated with trypsin: $RI_c$ and *bone propagation* did not change significantly after 4h of treatment, while $RI_b$ and *cartilage length* showed a small variation only after 4h. On the other hand, samples degraded with collagenase showed a considerable and progressive decrease in $RI_c$ and *cartilage length*, resulting in a total loss of cartilage after 24h. It was not possible to determine $RI_c$ at 24h due to the complete absence of the water-cartilage interface. $RI_b$ was not affected by collagenase degradation, while the *bone propagation* increased gradually, in line with the loss of the cartilage. Overall, these results revealed that collagenase had a more pronounced impact on the structure of the cartilage samples compared to trypsin, in agreement with literature findings at high frequency US [7], [24].

*Compressed features*

Figure 1c and Figure 2c report the results of the discriminant compressed features derived from RF data using encoder layers of an Auto Encoder (AE) neural network. The AE neural network allowed unsupervised learning and feature extraction [25]. It consisted of an encoder and decoder building blocks to reconstruct the output data from the input. Since 2014, with the development of deep learning techniques, the automatic extraction of compressed features using AE has found applications in several domains, such as pattern recognition, computer vision, data generation, recommender systems and fault detection systems [26] [27]. In the context of cartilage degeneration management, a standard AE was used to learn and extract the most useful discriminative features of knee OA from

pixel intensities in X-ray images [28]. In a different study, AE was used to generate new data for early known OA cases by combining informative features from grade 0 and grade 2 of Kellgren-Lawrence grading system [29]. However, to the best of our knowledge, the potential of AE has not been explored for characterizing cartilage data based on RF signals. In our study, we hypothesized that these compressed features would reveal changes in the cartilage samples as degradation progressed. Although dimensionless, the statistical analysis of these compressed features indicated that collagenase treatment induced more pronounced changes compared to trypsin treatment (see Figure 1c and Figure 2c), in agreement with the results highlighted by the above-mentioned metrics.

*ML-based classification*

In recent years, there has been a remarkable increase in the adoption of artificial intelligence (AI) for monitoring cartilage degeneration. These contributions extend to the classification of OA severity, lesion detection, cartilage segmentation, and the development of predictive models for knee OA progression [30]. Recent applications of deep learning in OA research involve the automatic detection of OA severity in radiographs and the identification of cartilage and meniscal lesions, as well as cartilage segmentation for T2 quantification in MR images. At the same time, applications of ML models have expanded to include the identification of individuals at high risk of developing OA using modifiable and non-modifiable risk factors such as obesity, genetic predisposition, joint injury, physical activity, and biomechanics [30]. ML models have also been developed using data from near-infrared spectroscopy to evaluate cartilage integrity during arthroscopy, enabling the distinction between healthy and diseased cartilage [31]. Moreover, in a recent study, ML and deep learning models were established by incorporating raw RF data alongside the average SoS value and T-score as QUS measurements, facilitating the creation of an in vivo automated system for osteoporosis classification and detection [32]. However, no previous ML applications have employed sets of relevant QUS features extracted from RF data to identify the degeneration status of cartilage tissue.

We developed for the first time six ML models using the seventeen relevant QUS metrics derived from RF data to automatically recognize healthy and degenerated cartilage samples. In Figure S2, the top informative features from each QUS dataset were reported; they could serve as promising indicators for predicting individual cartilage changes through the training of ML models. From the results, we found that the application of emerging ML models, such as the Ensemble model, to distinguish healthy and trypsin-degenerated cartilage, provided an *accuracy* and *AUC* of up to 80% and 75%, respectively (Table S2), while the logistic regression model yielded an *accuracy* and *AUC* of up to 93.33% and 90.00% for collagenase treatment (Table S3).

*Histological and mechanical analyses*

Figure 4 and Figure 5 clearly show that both trypsin and collagenase enzymes caused a progressive modification of the cartilage matrix and its mechanical properties. A significant decrease in both histological proteoglycan content and mechanical properties was found at each time point of the analysis, for both trypsin and collagenase. The histological and mechanical analyses further corroborated the findings of QUS parameters and ML classification: specifically, the impact of collagenase seemed more pronounced compared to trypsin. In particular, the trend in cartilage thickness calculated from RF data is consistent with the trend in cartilage thickness determined through histology. Trypsin had no effect on cartilage thickness since the collagen network was not affected (see Figure S5 in the supplementary material). In contrast, collagenase had a considerable impact on thickness, resulting in a significant decrease after 24 hours by both histological (75%) and US analysis (71%) (see Figure S5 in the supplementary material).

Similarly, the mechanical properties were more affected by collagenase compared to trypsin treatment. AFM results revealed a maximum decrease in the young modulus of cartilage of 77% after 4h of trypsin treatment. However, this effect was not evident in the acoustic properties of cartilage. Specifically, $RI_c$ did not exhibit a significant decrease after 4h of trypsin treatment, possibly owing to the high data variability or to the presence of an intact collagen network (as demonstrated by the histological results). The young modulus of the cartilage decreased by 99% after 24h of collagenase treatment. Accordingly, the water-cartilage interface disappeared in the RF signal, due to the complete degradation of cartilage, making infeasible the calculation of $RI_c$ after 24h of collagenase treatment.

These findings suggest that QUS metrics derived from RF data, selected based on their informative weights and coupled with ML models, offer the potential to serve as an automated and quantitative tool for cartilage monitoring. However, the amount of available training data in this study limited the fine discrimination of more than two classes of degradation (*i.e.*, three classes). To address this concern, future efforts may focus on enlarging the dataset with additional ex-vivo samples and optimizing ML models, *e.g.*, including a dedicated step to select the most informative features and the optimal model parameters.

## Conclusion

In this work, we performed a thorough analysis of radiofrequency signals acquired with a ultrasound transmission frequency equal to 15 MHz, with the aim of detecting changes in ex-vivo cartilage samples. Healthy bovine samples were chemically degraded using trypsin and collagenase enzymes, to simulate the loss of proteoglycans and collagen networks during degenerating pathologies, such as osteoarthritis. We extracted a total of seventeen quantitative ultrasound metrics, that were able to detect changes in the cartilage structure and variations in the complexity and regularity of the signals, due to the degradation process. The quantitative ultrasound metrics were used as input for machine learning models to automatically discriminate between healthy and degenerated cartilage samples. The quantitative ultrasound metrics and classifiers performed better with the collagenase treatment, as the effects on the tissue matrix were more pronounced, as confirmed by histological and mechanical findings. This work represents the first attempt to use quantitative ultrasound measures in conjunction with machine learning classifiers for assessing the cartilage status and paves the way to a future in vivo translation of this methodology.

## Materials and Methods

### Sample preparation and experimental setup

Four bovine condyles, without visible lesions, were bought from a nearby market. A bone biopsy instrument was used to extract 38 samples, each with a diameter of 6 mm and a length of 5/6 mm. Healthy specimens were initially scanned with US before undergoing enzymatic degradation with trypsin (n=20) and collagenase (n=18). For each treatment group, 4 samples were collected for subsequent histological analysis at the 0-hour mark. The specimens of the trypsin group were immersed in a 0.25% trypsin-ethylenediamtetra-acetic acid (EDTA) (59428C, Sigma Aldrich) solution at 37 °C, as described by Wang et *al*. [24]. After 2h and 4h of treatment, specimens were washed in a solution of 10× Phosphate Buffered Saline (PBS, P4417, Merck) and scanned to acquire RF data. At each time point, 4 samples were sacrificed for histological analysis. The specimens of the collagenase group were placed in a 4 mg/mL collagenase solution (SCR103, Sigma Aldrich), at 37 °C [24]. After 6h and 24h of treatment, specimens were washed in a solution of 10× PBS and scanned to acquire RF data. At each time point, 4 samples were sacrificed for histological analysis.

The experimental setup used to acquire RF data is described in [15], [16]. Basically, a support for the probe and a sample holder were immersed in a tank filled with deionized and degassed water. The sample holder included an agarose support with 6 mm diameter holes to host the cartilage samples. The agarose supports were prepared with a concentration of 2% w/v to prevent any interference with US beam, since it shows acoustic properties and echogenicity similar to water [33]. The RF data were acquired using the ArtUS EXT-1H system (Telemed, Italy) equipped with a 192 elements linear probe L15-7H40-A5 (7.5-15MHz), setting the transmission frequency to 15 MHz. A schematic representation of the experimental procedure is reported in Figure 6.

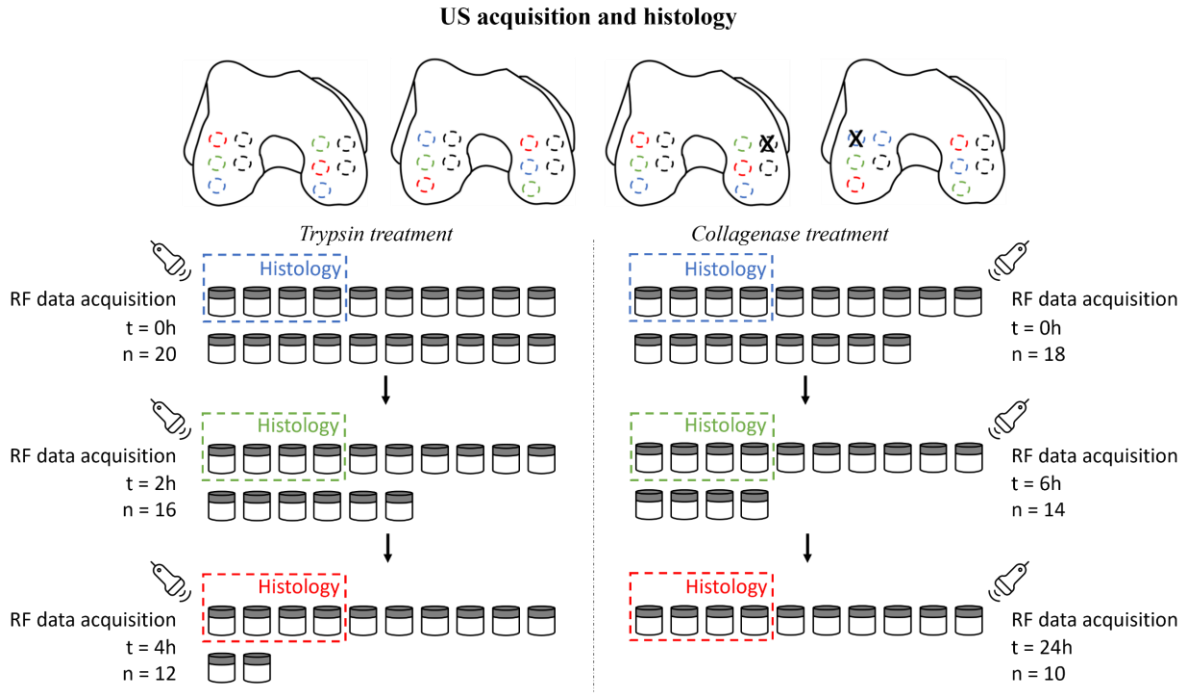


Figure 6 – Schematic representation of the experimental procedure. A total of 38 specimens were sampled from 4 bovine condyles and undergone to trypsin (n=20) and collagenase (n=18) treatment. Thre time points of evaluation were considered for trypsin (0h, 2h and 4h) and for collagenase (0h, 6h and 24h). At each time point, RF data were acquired and 4 samples were sacrificed for subsequent histological analysis.

In addition, a total of 23 cartilage samples were extracted from two different condyles to perform AFM analyses.

**Ultrasound data analysis**

In our study, a total of 90 RF acquisitions (48 for the trypsin treatment group and 42 for the collagenase treatment group consisting of 60 RF lines (columns) and 1036 samples (rows)) were processed off-line using python and Matlab software routines. To characterize the cartilage specimens at different time points of degradation, we extracted three sets of QUS metrics for each examined RF line: complexity and irregularity metrics, cartilage features, and compressed feature metrics.

The complexity and irregularity metrics (*approximate entropy* (*ApEn*), *sample entropy* (*sampEn*), *spectral entropy*, *mean crossing*, *katz fractal dimension*, *50$^{th}$ percentile*, *std*, *kurtosis*) were computed within a ROI ($ROI_1$) that includes the entire specimen (30 RF lines × 300 samples, see Figure 7a,b). The cartilage features were extracted in the central portion of each sample ($ROI_2$), where the main features of the sample are clearly visible (21 RF lines × 1036 samples, see Figure 7a,b). They include the RI at the water-cartilage surface ($RI_c$), RI at the cartilage-bone interface ($RI_b$), *bone propagation* (indicating how much the signal is spread after the bone interface) and the cartilage *cartilage length*

(calculated as the difference between the bone surface and the first signal peak). Finally, the compressed feature metrics (*F1, F2, F3, F4, F5*) were generated by applying encoder layers within an AE neural network, effectively condensing the data within $ROI_1$ (see Figure S1a).

The mathematical definition of the proposed QUS metrics is described in detail in the appendix section (a) of the supplementary material.

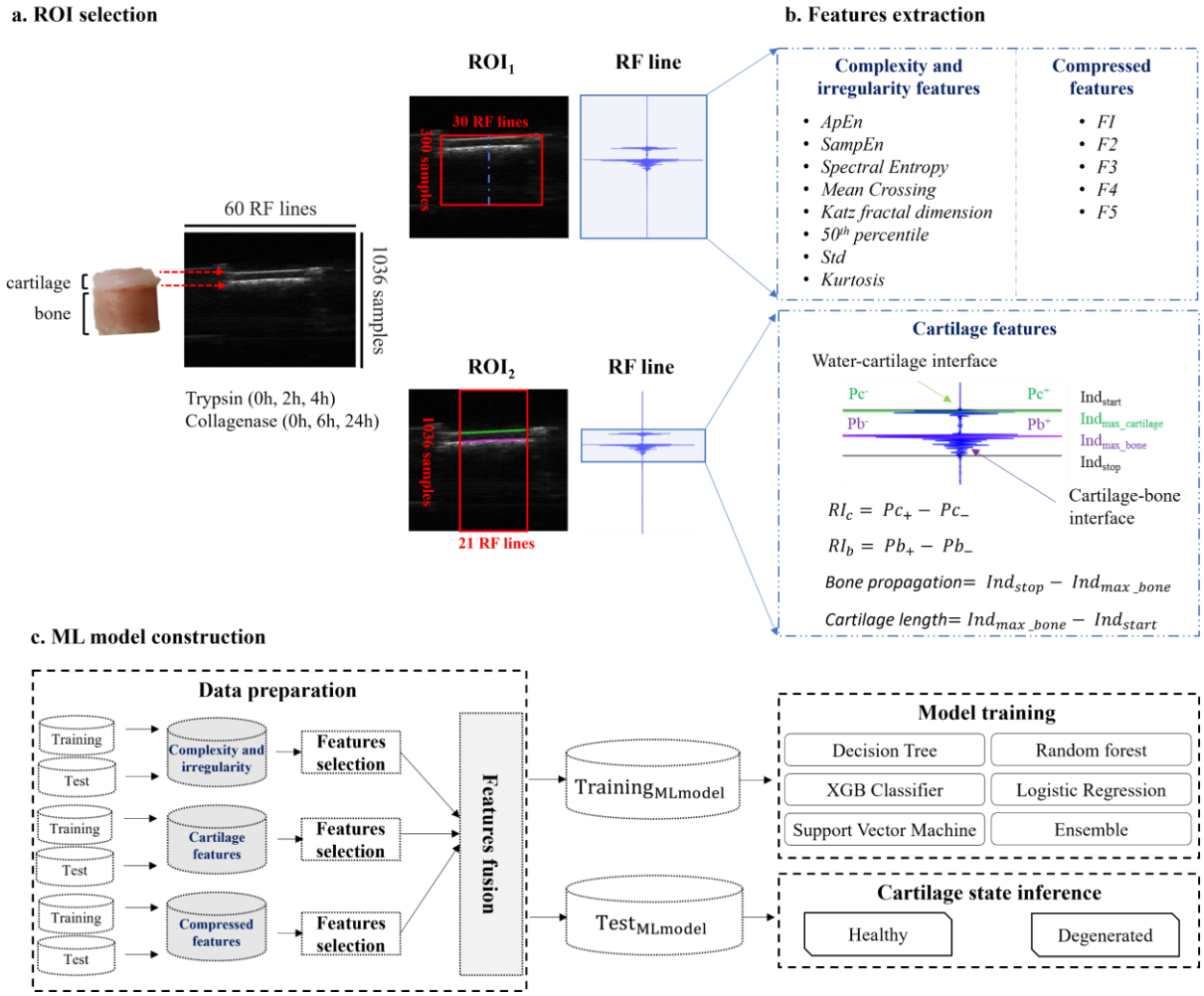


Figure 7 – Workflow for RF data analysis. In (a), a representative B-mode image is shown, highlighting the cartilage and bone interfaces. Two regions of interests were identified for future extraction: $ROI_1$, which includes the whole sample and $ROI_2$, in the middle of the sample to avoid irregular boundaries. Complexity and irregularity features and compressed features were calculated in $ROI_1$, while cartilage features were computed in $ROI_2$ (b). In (c), the workflow for ML model construction is represented. For each dataset (complexity and irregularity, cartilage features, compressed features), a feature selection step has been applied to extract the most informative features to build the ML models.

*ML-based classification*

*Data.* To construct the ML models, we allocated for the training phase 33 specimens from the trypsin treatment and 27 specimens from the collagenase group. To evaluate the performance of the models to distinguish healthy and degenerated samples, we allocated 15 specimens from both treatments (5 form "healthy group" and 10 from the "degenerated group").

*Data preparation.* In this step we normalized the data dividing each RF line data by its maximum absolute value [34]. Then, using the LinearSVC algorithm [35], we selected the features that exhibited a significant association with cartilage degeneration. Finally, we created the $Training_{MLmodel}$ and

$Test_{MLmodel}$ datasets for the trypsin and collagenase treatment group by concatenating the most informative features for each cartilage sample. A detailed description of this step, including data preprocessing, feature selection and feature fusion process is reported in the appendix section (b) of the supplementary material.

*Classification of the cartilage status.* The $Training_{MLmodel}$ datasets were used to train the ML models. In this study, we conducted experiments using six different models, namely the decision tree, XGB classifier, support vector machine, random forest, and logistic regression, as previously studied in [36]. Ensemble models were constructed when any individual ML model achieved an overall *accuracy* exceeding 90%. These ensemble models combined the predictions of the three top-performing single classifiers, with the final result determined through a majority voting mechanism [37].

*Evaluation metrics for ML models.* To assess the classifiers' ability to discriminate healthy from degenerated cartilage samples, we used the following evaluation metrics: *accuracy* ( $(T_p + T_n)/(T_p + F_n + T_n + F_p)$), *precision* ( $T_p/(T_p + F_p)$), *recall* ($T_p/(T_p + F_n)$), *F1-score* ((2 × (*recall* × *precision*)/(*recall* + *precision*)), and *AUC* metrics [30]. The parameters $T_p$, $T_n$, $F_p$, and $F_n$ refer to the healthy samples correctly classified as healthy one, degenerated samples correctly classified as degenerated ones, healthy samples classified as degenerated ones, and degenerated samples classified as healthy ones, respectively. *Accuracy* measures the ratio of correctly classified samples, *precision* quantifies the ratio of correctly classified healthy samples, *recall* measures the ratio of correctly classified healthy samples over the total number, *F1-score* combined accuracy and recall, and *AUC* assesses the model's capability to distinguish between classes.

**Histological analyses**

Osteochondral plugs were fixed in neutral buffered formalin (10%) for 24 hours, washed, placed into the decalcifying solution (MicroDecfast, Diapath S.p.A., Martinengo, BG, Italy) for 6 days, dehydrated in graded concentrations of ethanol and embedded in paraffin. As shown in supplementary Figure S6a, serial sections of 5 µm were obtained longitudinal to the osteochondral plugs in three different areas defined as α, β, and γ. Fifteen slices were obtained from each area, equally spaced from each other, to evaluate the centre of the sample. Sections were stained with Safranin O for 10 minutes and Fast Green for 3 minutes (both from Sigma Aldrich-Merck). Picrosirius Red staining was also performed using 0,1% Direct Red 80 in saturated picric acid in $H_2O$ for 60 minutes (Sigma Aldrich-Merck). Images were captured using an Eclipse 90i microscope (Nikon Instruments Europe BV) equipped with a CCD camera. Two independent observers selected the total cartilage area, Safranin O and Picrosirius Red positive areas of the cartilage by using the dedicated Software NIS-Elements that expressed the selected area as $\mu m^2$. As shown in supplementary Figure S6b, c, the percentage of positive area was calculated as the ratio between total and positive area [38].

**AFM indentation**

AFM indentation [39] was performed employing a Nanowizard IV AFM system (Bruker, USA), mounted on a DMi8 inverted optical microscope (Leica Microsystem, Germany). Silicon nitride triangular cantilever (DNP, Bruker, USA) with a nominal spring constant of 0.24 N/m, equipped with a pyramidal probe with a typical tip radius of 20 nm were used for cartilage indentation. The actual spring constant was evaluated per each cantilever using the thermal noise method [40].

The samples were cleaned with PBS (Sigma-Aldrich, USA) and then placed in a Teflon sample holder, designed and fabricated for this purpose (see the supplementary Figure S7) and filled with PBS buffer for the experiment.

Indentations were performed on untreated samples and then repeated on the same samples after the treatment with trypsin (19 samples) and collagenase (4 samples) performed in situ exploiting the custom-made Teflon holder. The different number of samples analyzed in the two treatment conditions is because, in the collagenase treatment group, the cartilages exhibited high adhesive gel-like properties upon treatment. Consequently, in some cases, the AFM probe, after indenting the sample, was still attached to the sample at the end of the force-distance (F-D) curve cycle. In such cases, the F-D curves did not conform with the contact criteria of the Hertz-Sneddon model, making impossible to fit the curve and determine the Young's modulus of elasticity (see Figure S4 in the supplementary material). As a result, the total number of analyzed samples treated by collagenase enzyme was reduced if compared with the samples treated with trypsin.

Three areas of 10x10 $\mu m^2$ were tested per each sample. In each region, 400 F-D curves [41] were acquired; in total 1200 curves per sample. The maximum force applied was 10 nN and the tip velocity was maintained 3 µm/s.

The data were analyzed with a built-in software (Bruker, USA) using the Bilodeau formula for a regular pyramidal punch [42] that extends the Hertz-model contact mechanics to the case of non-axisymmetric indenters.

### Statistical analysis

Statistical comparisons between all experimental groups were performed using non-parametric tests, based on the non-normal distribution of histological, mechanical and RF data. All the data were analyzed applying a non-parametric Kruskal-Wallis test for multiple comparisions, while Dunn's test was used for post hoc analyses. A p-value smaller than 0.05 was deemed as significant (*).

## ACKNOWLEDGMENTS

This work received funding from the European Union's Horizon 2020 research and innovation program, grant agreement No 814413, project ADMAIORA (ADvanced nanocomposite MAterIals fOr in situ treatment and ultRAsound-mediated management of osteoarthritis). The authors would like to express their great appreciation to Angelo, from the Antica Macelleria Cafarelli, for providing us with the ex-vivo samples.

### Ethics approval not required

# REFERENCES


[1] A. J. Sophia Fox, A. Bedi, and S. A. Rodeo, “The basic science of articular cartilage: Structure, composition, and function,” *Sports Health*, vol. 1, no. 6, pp. 461–468, 2009, doi: 10.1177/1941738109350438.

[2] F. Daou, A. Cochis, M. Leigheb, and L. Rimondini, “Current Advances in the Regeneration of Degenerated Articular Cartilage: A Literature Review on Tissue Engineering and Its Recent Clinical Translation,” *Materials*, vol. 15, no. 1, p. 31, Dec. 2021, doi: 10.3390/ma15010031.

[3] M. L’Hermette, C. Tourny-Chollet, G. Polle, and F. Dujardin, “Articular Cartilage, Degenerative Process, and Repair: Current Progress,” *Int J Sports Med*, vol. 27, no. 9, pp. 738–744, Sep. 2006, doi: 10.1055/s-2005-872824.

[4] R. J. Daher, N. O. Chahine, A. S. Greenberg, N. A. Sgaglione, and D. A. Grande, “New methods to diagnose and treat cartilage degeneration,” *Nat Rev Rheumatol*, vol. 5, no. 11, pp. 599–607, Nov. 2009, doi: 10.1038/nrrheum.2009.204.

[5] M. L. Oelze and J. Mamou, “Review of Quantitative Ultrasound: Envelope Statistics and Backscatter Coefficient Imaging and Contributions to Diagnostic Ultrasound,” *IEEE Trans Ultrason Ferroelectr Freq Control*, vol. 63, no. 2, pp. 336–351, 2016, doi: 10.1109/TUFFC.2015.2513958.

[6] S. Z. Wang, Y. P. Huang, S. Saarakkala, and Y. P. Zheng, “Quantitative Assessment of Articular Cartilage with Morphologic, Acoustic and Mechanical Properties Obtained Using High-Frequency Ultrasound,” *Ultrasound Med Biol*, vol. 36, no. 3, pp. 512–527, 2010, doi: 10.1016/j.ultrasmedbio.2009.12.005.

[7] S. Saarakkala, J. Töyräs, J. Hirvonen, M. S. Laasanen, R. Lappalainen, and J. S. Jurvelin, “Ultrasonic quantitation of superficial degradation of articular cartilage,” *Ultrasound Med Biol*, vol. 30, no. 6, pp. 783–792, Jun. 2004, doi: 10.1016/j.ultrasmedbio.2004.03.005.

[8] Q. Wang *et al.*, “Real-Time Ultrasonic Assessment of Progressive Proteoglycan Depletion in Articular Cartilage,” *Ultrasound Med Biol*, vol. 34, no. 7, pp. 1085–1092, Jul. 2008, doi: 10.1016/j.ultrasmedbio.2007.12.006.

[9] H. J. Nieminen *et al.*, “Real-time ultrasound analysis of articular cartilage degradation in vitro,” *Ultrasound Med Biol*, vol. 28, no. 4, pp. 519–525, Apr. 2002, doi: 10.1016/S0301-5629(02)00480-5.

[10] E. Kaleva, S. Saarakkala, J. Töyräs, H. J. Nieminen, and J. S. Jurvelin, “In-Vitro Comparison of Time-Domain, Frequency-Domain and Wavelet Ultrasound Parameters in Diagnostics of Cartilage Degeneration,” *Ultrasound Med Biol*, vol. 34, no. 1, pp. 155–159, Jan. 2008, doi: 10.1016/j.ultrasmedbio.2007.06.028.

[11] T. H. Lye *et al.*, “Quantitative Ultrasound Assessment of Early Osteoarthritis in Human Articular Cartilage Using a High-Frequency Linear Array Transducer,” *Ultrasound Med Biol*, vol. 48, no. 8, pp. 1429–1440, Aug. 2022, doi: 10.1016/j.ultrasmedbio.2022.03.006.

[12] H. J. Niu, Q. Wang, Y. X. Wang, D. Y. Li, Y. B. Fan, and W. F. Chen, “Ultrasonic reflection coefficient and surface roughness index of OA articular cartilage: Relation to pathological assessment,” *BMC Musculoskelet Disord*, vol. 13, 2012, doi: 10.1186/1471-2474-13-34.

[13] J. Zhang, L. Xiao, L. Tong, C. Wan, and Z. Hao, “Quantitative Evaluation of Enzyme-Induced Porcine Articular Cartilage Degeneration Based on Observation of Entire Cartilage Layer Using Ultrasound,”

*Ultrasound Med Biol*, vol. 44, no. 4, pp. 861–871, Apr. 2018, doi: 10.1016/j.ultrasmedbio.2017.11.016.

[14] Y. T. K. Hattori, K. Ikeuchi, Y. Morita, "Quantitative ultrasonic assessment for detecting microscopic cartilage damage in osteoarthritis," *Arthritis Res Ther*, vol. 7, no. 1, pp. 1–9, 2004, doi: 10.1186/ar1463.

[15] A. Sorriento, A. Poliziani, A. Cafarelli, G. Valenza, and L. Ricotti, "A novel quantitative and reference-free ultrasound analysis to discriminate different concentrations of bone mineral content," *Sci Rep*, vol. 11, no. 1, pp. 1–14, 2021, doi: 10.1038/s41598-020-79365-0.

[16] A. Sorriento; A. Cafarelli; G. Valenza; L. Ricotti, "Ex-vivo quantitative ultrasound assessment of cartilage degeneration.," in *Annu Int Conf IEEE Eng Med Biol Soc.*, 2021, pp. 2976–2980. doi: 10.1109/EMBC46164.2021.9630198.

[17] H. Wang, C. Wu, T. Li, Y. He, P. Chen, and A. Bezerianos, "Driving Fatigue Classification Based on Fusion Entropy Analysis Combining EOG and EEG," *IEEE Access*, vol. 7, pp. 61975–61986, 2019, doi: 10.1109/ACCESS.2019.2915533.

[18] Ji, Ma, Dong, and Zhang, "EEG Signals Feature Extraction Based on DWT and EMD Combined with Approximate Entropy," *Brain Sci*, vol. 9, no. 8, p. 201, Aug. 2019, doi: 10.3390/brainsci9080201.

[19] C. CANYURT and R. ZENGİN, "Epileptic Activity Detection using Mean Value, RMS, Sample Entropy, and Permutation Entropy Methods," *The Journal of Cognitive Systems*, Jun. 2023, doi: 10.52876/jcs.1226579.

[20] M. E. H. Chowdhury *et al.*, "Wearable Real-Time Heart Attack Detection and Warning System to Reduce Road Accidents," *Sensors*, vol. 19, no. 12, p. 2780, Jun. 2019, doi: 10.3390/s19122780.

[21] J. Mekyska *et al.*, "Robust and complex approach of pathological speech signal analysis," *Neurocomputing*, vol. 167, pp. 94–111, Nov. 2015, doi: 10.1016/j.neucom.2015.02.085.

[22] B. S. Raghavendra and D. Narayana Dutt, "A note on fractal dimensions of biomedical waveforms," *Comput Biol Med*, vol. 39, no. 11, pp. 1006–1012, Nov. 2009, doi: 10.1016/j.compbiomed.2009.08.001.

[23] R. Karpiński, P. Krakowski, J. Jonak, A. Machrowska, M. Maciejewski, and A. Nogalski, "Diagnostics of Articular Cartilage Damage Based on Generated Acoustic Signals Using ANN—Part II: Patellofemoral Joint," *Sensors*, vol. 22, no. 10, p. 3765, May 2022, doi: 10.3390/s22103765.

[24] S.-Z. Wang, Y.-P. Huang, S. Saarakkala, and Y.-P. Zheng, "Quantitative Assessment of Articular Cartilage with Morphologic, Acoustic and Mechanical Properties Obtained Using High-Frequency Ultrasound," *Ultrasound Med Biol*, vol. 36, no. 3, pp. 512–527, Mar. 2010, doi: 10.1016/j.ultrasmedbio.2009.12.005.

[25] H. Bourlard and Y. Kamp, "Auto-association by multilayer perceptrons and singular value decomposition," *Biol Cybern*, vol. 59, no. 4–5, pp. 291–294, Sep. 1988, doi: 10.1007/BF00332918.

[26] S. Chen and W. Guo, "Auto-Encoders in Deep Learning—A Review with New Perspectives," *Mathematics*, vol. 11, no. 8, p. 1777, Apr. 2023, doi: 10.3390/math11081777.

[27] Y. Liu *et al.*, "Fault diagnosis approach for photovoltaic array based on the stacked auto-encoder and clustering with I-V curves," *Energy Convers Manag*, vol. 245, p. 114603, Oct. 2021, doi: 10.1016/j.enconman.2021.114603.

[28] Y. Nasser, R. Jennane, A. Chetouani, E. Lespessailles, and M. El Hassouni, “Discriminative Regularized Auto-Encoder for Early Detection of Knee OsteoArthritis: Data from the Osteoarthritis Initiative,” *IEEE Trans Med Imaging*, vol. 39, no. 9, pp. 2976–2984, Sep. 2020, doi: 10.1109/TMI.2020.2985861.

[29] R. J. Zhe Wang, A. Chetouani, “Key-Exchange Convolutional Auto-Encoder for Data Augmentation in Early Knee OsteoArthritis Classification,” *ArXiv*, vol. 2302, p. 13336, 2023.

[30] G. B. Joseph, C. E. McCulloch, J. H. Sohn, V. Pedoia, S. Majumdar, and T. M. Link, “AI MSK clinical applications: cartilage and osteoarthritis,” *Skeletal Radiol*, vol. 51, no. 2, pp. 331–343, Feb. 2022, doi: 10.1007/s00256-021-03909-2.

[31] I. O. Afara *et al.*, “Machine Learning Classification of Articular Cartilage Integrity Using Near Infrared Spectroscopy,” *Cell Mol Bioeng*, vol. 13, no. 3, pp. 219–228, Jun. 2020, doi: 10.1007/s12195-020-00612-5.

[32] W. Luo *et al.*, “Osteoporosis Diagnostic Model Using a Multichannel Convolutional Neural Network Based on Quantitative Ultrasound Radiofrequency Signal,” *Ultrasound Med Biol*, vol. 48, no. 8, pp. 1590–1601, Aug. 2022, doi: 10.1016/j.ultrasmedbio.2022.04.005.

[33] A. Cafarelli, A. Verbeni, A. Poliziani, P. Dario, A. Menciassi, and L. Ricotti, “Tuning acoustic and mechanical properties of materials for ultrasound phantoms and smart substrates for cell cultures,” *Acta Biomater*, 2017, doi: 10.1016/j.actbio.2016.11.049.

[34] A. H. Seno, Z. Sharif Khodaei, and M. H. F. Aliabadi, “Passive sensing method for impact localisation in composite plates under simulated environmental and operational conditions,” *Mech Syst Signal Process*, vol. 129, pp. 20–36, Aug. 2019, doi: 10.1016/j.ymssp.2019.04.023.

[35] D. Zhang *et al.*, “Heart Disease Prediction Based on the Embedded Feature Selection Method and Deep Neural Network,” *J Healthc Eng*, vol. 2021, pp. 1–9, Sep. 2021, doi: 10.1155/2021/6260022.

[36] B. Mahesh, “Machine learning algorithms-a review,” *International Journal of Science and Research (IJSR)*, vol. 9.1, pp. 381–386, 2020, doi: 10.21275/ART20203995.

[37] A. Dogan and D. Birant, “A Weighted Majority Voting Ensemble Approach for Classification,” in *2019 4th International Conference on Computer Science and Engineering (UBMK)*, IEEE, Sep. 2019, pp. 1–6. doi: 10.1109/UBMK.2019.8907028.

[38] L. Qin, Y. Zheng, C. Leung, A. Mak, W. Choy, and K. Chan, “Ultrasound detection of trypsin-treated articular cartilage: its association with cartilaginous proteoglycans assessed by histological and biochemical methods,” *J Bone Miner Metab*, vol. 20, no. 5, pp. 281–287, Sep. 2002, doi: 10.1007/s007740200040.

[39] S. Kerdegari *et al.*, “Insights in Cell Biomechanics through Atomic Force Microscopy,” *Materials*, vol. 16, no. 8, p. 2980, Apr. 2023, doi: 10.3390/ma16082980.

[40] J. L. Hutter and J. Bechhoefer, “Calibration of atomic-force microscope tips,” *Review of Scientific Instruments*, vol. 64, no. 7, pp. 1868–1873, Jul. 1993, doi: 10.1063/1.1143970.

[41] B. Cappella, P. Baschieri, C. Frediani, P. Miccoli, and C. Ascoli, “Force-distance curves by AFM,” *IEEE Engineering in Medicine and Biology Magazine*, vol. 16, no. 2, pp. 58–65, 1997, doi: 10.1109/51.582177.

[42] G. G. Bilodeau, “Regular Pyramid Punch Problem,” *J Appl Mech*, vol. 59, no. 3, pp. 519–523, Sep. 1992, doi: 10.1115/1.2893754.